

# Rational design of cationic lipids for siRNA delivery

Sean C Semple<sup>1,6</sup>, Akin Akinc<sup>2,6</sup>, Jianxin Chen<sup>1,5</sup>, Ammen P Sandhu<sup>1</sup>, Barbara L Mui<sup>1,5</sup>, Connie K Cho<sup>1</sup>, Dinah W Y Sah<sup>2</sup>, Derrick Stebbing<sup>1</sup>, Erin J Crosley<sup>1</sup>, Ed Yaworski<sup>1</sup>, Ismail M Hafez<sup>3</sup>, J Robert Dorkin<sup>2</sup>, June Qin<sup>2</sup>, Kieu Lam<sup>1</sup>, Kallanthottathil G Rajeev<sup>2</sup>, Kim F Wong<sup>3</sup>, Lloyd B Jeffs<sup>1</sup>, Lubomir Nechev<sup>2</sup>, Merete L Eisenhardt<sup>1</sup>, Muthusamy Jayaraman<sup>2</sup>, Mikameh Kazem<sup>3</sup>, Martin A Maier<sup>2</sup>, Masuna Srinivasulu<sup>4</sup>, Michael J Weinstein<sup>2</sup>, Qingmin Chen<sup>2</sup>, Rene Alvarez<sup>2</sup>, Scott A Barros<sup>2</sup>, Soma De<sup>2</sup>, Sandra K Klimuk<sup>1</sup>, Todd Borland<sup>2</sup>, Verbena Kosovrasti<sup>2</sup>, William L Cantley<sup>2</sup>, Ying K Tam<sup>1,5</sup>, Muthiah Manoharan<sup>2</sup>, Marco A Ciufolini<sup>4</sup>, Mark A Tracy<sup>2</sup>, Antonin de Fougerolles<sup>2</sup>, Ian MacLachlan<sup>1</sup>, Pieter R Cullis<sup>3</sup>, Thomas D Madden<sup>1,5</sup> & Michael J Hope<sup>1,5</sup>

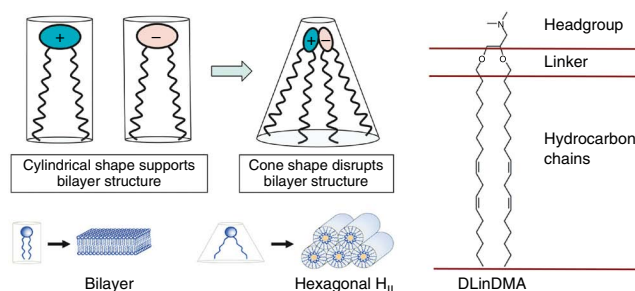
**We adopted a rational approach to design cationic lipids for use in formulations to deliver small interfering RNA (siRNA). Starting with the ionizable cationic lipid 1,2-dilinolexyloxy-3-dimethylaminopropane (DLinDMA), a key lipid component of stable nucleic acid lipid particles (SNALP) as a benchmark, we used the proposed *in vivo* mechanism of action of ionizable cationic lipids to guide the design of DLinDMA-based lipids with superior delivery capacity. The best-performing lipid recovered after screening (DLin-KC2-DMA) was formulated and characterized in SNALP and demonstrated to have *in vivo* activity at siRNA doses as low as 0.01 mg/kg in rodents and 0.1 mg/kg in nonhuman primates. To our knowledge, this represents a substantial improvement over previous reports of *in vivo* endogenous hepatic gene silencing.**

A key challenge in realizing the full potential of RNA interference (RNAi) therapeutics is the efficient delivery of siRNA, the molecules that mediate RNAi. The physicochemical characteristics of siRNA—high molecular weight, anionic charge and hydrophilicity—prevent passive diffusion across the plasma membrane of most cell types. Therefore, delivery mechanisms are required that allow siRNA to enter cells, avoid endolysosomal compartmentalization and localize in the cytoplasm where it can be loaded into the RNA-induced

silencing complex. To date, formulation in lipid nanoparticles (LNPs) represents one of the most widely used strategies for *in vivo* delivery of siRNA<sup>1,2</sup>. LNPs represent a class of particles comprised of different lipid compositions and ratios as well as different sizes and structures formed by different methods. A family of LNPs, SNALP<sup>3–6</sup>, is characterized by very high siRNA-encapsulation efficiency and small, uniformly sized particles, enabled by a controlled step-wise dilution methodology. LNPs, including SNALP, have been successfully used to silence therapeutically relevant genes in nonhuman primates<sup>6–8</sup> and are currently being evaluated in several clinical trials.

An empirical, combinatorial chemistry-based approach recently identified novel materials for use in LNP systems<sup>7</sup>. A key feature of this approach was the development of a one-step synthetic strategy that allowed the rapid generation of a diverse library of ~1,200 compounds. This library was then screened for novel materials capable of mediating efficient delivery of siRNA *in vitro* and *in vivo*. Here, we instead used a medicinal chemistry (that is, structure-activity relationship) approach, guided by the putative *in vivo* mechanism of action of ionizable cationic lipids, for rational lipid design. Specifically, we hypothesized that after endocytosis, the cationic lipid interacts with naturally occurring anionic phospholipids in the endosomal membrane, forming ion pairs that adopt nonbilayer structures and disrupt membranes (Fig. 1)<sup>9–12</sup>. We previously advanced the concept

**Figure 1** Proposed mechanism of action for membrane disruptive effects of cationic lipids and structural diagram of DLinDMA divided into headgroup, linker and hydrocarbon chain domains. In isolation, cationic lipids and endosomal membrane anionic lipids such as phosphatidylserine adopt a cylindrical molecular shape, which is compatible with packing in a bilayer configuration. However, when cationic and anionic lipids are mixed together, they combine to form ion pairs where the cross-sectional area of the combined headgroup is less than that of the sum of individual headgroup areas in isolation. The ion pair therefore adopts a molecular 'cone' shape, which promotes the formation of inverted, nonbilayer phases such as the hexagonal H<sub>II</sub> phase illustrated. Inverted phases do not support bilayer structure and are associated with membrane fusion and membrane disruption<sup>9,21</sup>.



<sup>1</sup>Tekmira Pharmaceuticals, Burnaby, British Columbia, Canada. <sup>2</sup>Alnylam Pharmaceuticals, Cambridge, Massachusetts, USA. <sup>3</sup>Department of Biochemistry and Molecular Biology and <sup>4</sup>Department of Chemistry, University of British Columbia, Vancouver, British Columbia, Canada. <sup>5</sup>Present address: Alkana Technologies, Vancouver, British Columbia, Canada. <sup>6</sup>These authors contributed equally to this work. Correspondence should be addressed to S.C.S. (ssemple@tekmirapharm.com) or A.A. (aakinc@alnylam.com).

Received 16 September 2009; accepted 17 December 2009; published online 17 January 2010; doi:10.1038/nbt.1602



**Table 1** Biophysical parameters and *in vivo* activities of LNPs containing novel lipids

Cationic lipid	Apparent lipid $pK_a^a$	$L_{II}$ to $H_{II}$ phase transition temperature ( $^{\circ}C$ ) <sup>b</sup>	<i>In vivo</i> ED <sub>50</sub> (mg/kg)
DLinDMA	6.8 ± 0.10	27	~1
DLinDAP	6.2 ± 0.05	26	40–50
DLin-K-DMA	5.9 ± 0.03	19	~0.4
DLin-KC2-DMA	6.7 ± 0.08	20	~0.1
DLin-KC3-DMA	7.2 ± 0.05	18	~0.6
DLin-KC4-DMA	7.3 ± 0.07	18	>3

<sup>a</sup> $pK_a$  values ± s.d. ( $n = 3$  to  $9$ ). <sup>b</sup> $L_{II}$  to  $H_{II}$  phase transition was measured at pH 4.8 in equimolar mixtures with DSPS, using differential scanning calorimetric, repeat scans reproducible to within 0.1  $^{\circ}C$ .

affect both the  $pK_a$  of the amine headgroup as well as the distance and flexibility of the charge presentation relative to the lipid bilayer interface. Inserting a single additional methylene group into the headgroup (DLin-KC2-DMA) produced a dramatic increase in potency relative to DLin-K-DMA. The ED<sub>50</sub> for this lipid was ~0.1 mg/kg, making it fourfold more potent than DLin-K-DMA and tenfold more potent than the DLinDMA benchmark when compared head-to-head in the Factor VII model (Fig. 2a). Further extension of the tether with additional methylene groups, however, substantially decreased activity, with an ED<sub>50</sub> of ~0.6 mg/kg for DLin-KC3-DMA and >3 mg/kg for DLin-KC4-DMA (Fig. 2b).

As changes in lipid design and chemistry may affect the pharmacokinetics, target tissue accumulation and intracellular delivery of LNP formulations, we investigated the relative importance of these parameters on LNP activity at an early stage in this research program. Several of the novel lipids were incorporated into LNP-siRNA formulations containing cyanine dye (Cy3)-labeled siRNA. Plasma, liver and spleen levels of siRNA were determined at 0.5 and 3 h after injection at siRNA doses of 5 mg/kg, and the results are presented in Supplementary Table 3. In general, formulations that were the most active in the mouse Factor VII screens achieved the highest liver levels of siRNA at 0.5 h; however, delivery of siRNA to the target tissue was not the primary factor responsible for activity. This is supported by the observations that most formulations accumulated in the liver and spleen quite quickly and that some formulations with similar liver levels of siRNA had large differences in activity. Moreover, plasma pharmacokinetics alone did not predict activity. For example, although DLin-KC2-DMA and DLinDMA had virtually indistinguishable blood pharmacokinetic profiles in mice (data not shown), the activity of DLin-KC2-DMA in LNPs is approximately tenfold greater than the

same formulation with DLinDMA. Taken together, these results led us to conclude that rapid target tissue accumulation was important, but not sufficient, for activity. Moreover, other parameters were more critical for maximizing the activity of LNP-siRNA formulations.

Two important parameters underlying lipid design for SNALP-mediated delivery are the  $pK_a$  of the ionizable cationic lipid and the abilities of these lipids, when protonated, to induce a nonbilayer (hexagonal  $H_{II}$ ) phase structure when mixed with anionic lipids. The  $pK_a$  of the ionizable cationic lipid determines the surface charge on the LNP under different pH conditions. The charge state at physiologic pH (e.g., in circulation) can influence plasma protein adsorption, blood clearance and tissue distribution behavior<sup>16</sup>, whereas the charge state at acidic pH (e.g., in endosomes) can influence the ability of the LNP to combine with endogenous anionic lipids to form endosomolytic nonbilayer structures<sup>9</sup>. Consequently, the ability of these lipids to induce  $H_{II}$  phase structure in mixtures with anionic lipids is a measure of their bilayer-destabilizing capacity and relative endosomolytic potential.

The fluorescent probe 2-(*p*-toluidino)-6-naphthalene sulfonic acid (TNS), which exhibits increased fluorescence in a hydrophobic environment, can be used to assess surface charge on lipid bilayers. Titrations of surface charge as a function of pH can then be used to determine the apparent  $pK_a$  of the lipid in the bilayer (hereafter referred to as  $pK_a$ ) of constituent lipids<sup>17</sup>. Using this approach, the  $pK_a$  values for LNPs containing DLinDAP, DLinDMA, DLin-K-DMA, DLin-KC2-DMA, DLin-KC3-DMA and DLin-KC4-DMA were determined (Table 1). The relative ability of the protonated form of the ionizable cationic lipids to induce  $H_{II}$  phase structure in anionic lipids was ascertained by measuring the bilayer-to-hexagonal  $H_{II}$  transition temperature ( $T_{BH}$ ) in equimolar mixtures with distearoylphosphatidylserine (DSPS) at pH 4.8, using <sup>31</sup>P NMR<sup>18</sup> and differential scanning calorimetric analyses<sup>19</sup>. Both techniques gave similar results.

The data presented in Table 1 indicate that the highly active lipid DLin-KC2-DMA has  $pK_a$  and  $T_{BH}$  values that are theoretically favorable for use in siRNA delivery systems. The  $pK_a$  of 6.4 indicates that LNPs based on DLin-KC2-DMA have limited surface charge in circulation, but will become positively charged in endosomes. Further, the  $T_{BH}$  for DLin-KC2-DMA is 7  $^{\circ}C$  lower than that for DLinDMA, suggesting that this lipid has improved capacity for destabilizing bilayers. However, the data also demonstrate that  $pK_a$  and  $T_{BH}$  do not fully account for the *in vivo* activity of lipids used in LNPs. For example, although DLin-KC3-DMA and DLin-KC4-DMA have identical  $pK_a$  and  $T_{BH}$  values, DLin-KC4-DMA requires a more than fivefold higher dose to achieve the same activity *in vivo*. Moreover,

**Figure 3** Efficacy of KC2-SNALP in rodents and nonhuman primates. (a) Improved efficacy of KC2-SNALP relative to the initial screening formulation tested in mice. The *in vivo* efficacy of KC2-SNALP (○) was compared to that of the unoptimized DLin-KC2-DMA screening (that is, PFV) formulation (●) in the mouse Factor VII model. Data points are expressed as a percentage of PBS control animals and represent group mean ( $n = 5$ ) ± s.d. (b) Efficacy of KC2-SNALP in nonhuman primates. Cynomolgus monkeys ( $n = 3$  per group) received a total dose of either 0.03, 0.1, 0.3 or 1 mg/kg siTTR, or 1 mg/kg siApoB formulated in KC2-SNALP or PBS as 15-min intravenous infusions (5 ml/kg) through the cephalic vein. Animals were euthanized 48 h after administration. *TTR* mRNA levels relative to *GAPDH* mRNA levels were determined in liver samples. Data points represent group mean ± s.d. \*,  $P < 0.05$ ; \*\*,  $P < 0.005$ .

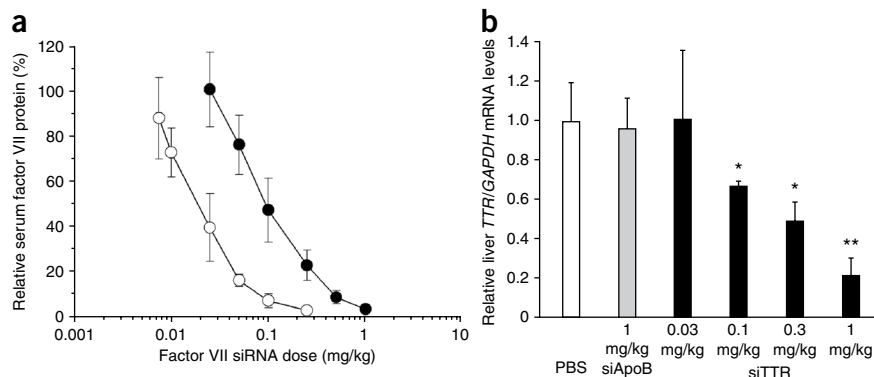


**Table 2 Clinical chemistry and hematology parameters for KC2-SNALP-treated rats**

Vehicle	siRNA dose (mg/kg) <sup>a</sup>	ALT (U/L)	AST (U/L)	Total Bilirubin (mg/dl)	BUN (mg/dl)	RBC ( $\times 10^6/\mu\text{l}$ )	Hemoglobin (g/dl)	WBC ( $\times 10^3/\mu\text{l}$ )	PLT ( $\times 10^3/\mu\text{l}$ )
PBS		56 $\pm$ 16	109 $\pm$ 31	2 $\pm$ 0	4.8 $\pm$ 0.8	5.5 $\pm$ 0.3	11.3 $\pm$ 0.4	11 $\pm$ 3	1,166 $\pm$ 177
KC2-SNALP	1	58 $\pm$ 22	100 $\pm$ 14	2 $\pm$ 0	4.4 $\pm$ 0.6	5.6 $\pm$ 0.2	11.6 $\pm$ 0.6	13 $\pm$ 2	1,000 $\pm$ 272
KC2-SNALP	2	73 $\pm$ 9	81 $\pm$ 10	2.2 $\pm$ 0.4	4.3 $\pm$ 0.6	5.9 $\pm$ 0.3	11.6 $\pm$ 0.3	13 $\pm$ 4	1,271 $\pm$ 269
KC2-SNALP	3	87 $\pm$ 19	100 $\pm$ 30	2 $\pm$ 0	5.0 $\pm$ 0.8	6.0 $\pm$ 0.2	11.9 $\pm$ 0.4	15 $\pm$ 2	958 $\pm$ 241

<sup>a</sup>Nontargeting, luciferase siRNA. Sprague-Dawley rats ( $n = 5$ ) received 15-min intravenous infusions of KC2-SNALP formulated siRNA at different dose levels. Blood samples were taken 24 h after administration. ALT, alanine aminotransferase; AST, aspartate aminotransferase; BUN, blood urea nitrogen; RBC, red blood cells; WBC, white blood cells; PLT, platelets.

DLin-KC2-DMA and DLin-KC4-DMA, which have very similar  $pK_a$  and  $T_{BH}$  values, exhibit a >30-fold difference in *in vivo* activity. This result suggests that other parameters, such as the distance and flexibility of the charged group relative to the lipid bilayer interface, may also be important. Thus, although the biophysical parameters of  $pK_a$  and  $T_{BH}$  are useful for guiding lipid design, the results presented in **Table 1** support the strategy of testing variants of lead lipids, even ones with very similar  $pK_a$  and  $T_{BH}$  values.

The lipid composition chosen for the initial formulation and screening of novel ionizable cationic lipids (cationic lipid/DSPC/cholesterol/PEG-lipid = 40:10:40:10 mol/mol, siRNA/total lipid ~ 0.05 wt/wt) was useful for determining the rank-order potency of novel lipids, but is not necessarily optimal for *in vivo* delivery. In addition, the *in vivo* activity of resultant LNP-siRNA formulations is affected by the formulation process employed and the resulting particle structure. Improvements in activity were possible with the preformed vesicle process by modifying and optimizing lipid ratios and formulation conditions (results not shown). However, we chose to further validate DLin-KC2-DMA activity specifically in the context of the SNALP platform, currently the most advanced LNP formulation for delivery of siRNA *in vivo*. We therefore tested *in vivo* a version of SNALP (termed KC2-SNALP), which uses less PEG lipid than reported previously<sup>6</sup> and in which DLinDMA was replaced with DLin-KC2-DMA. The incorporation of DLin-KC2-DMA into SNALP led to a marked improvement in potency in the mouse Factor VII model; the measured  $ED_{50}$  decreased from ~0.1 mg/kg for the unoptimized screening formulation to ~0.02 mg/kg for the KC2-SNALP formulation (**Fig. 3a**). KC2-SNALP also exhibited similar potency in rats (data not shown). Furthermore, after a single administration in rats, KC2-SNALP-mediated gene silencing was found to persist for over 10 d (**Supplementary Fig. 1**).

In addition to efficacy, tolerability is another critical attribute of a suitable LNP-siRNA delivery system for human use. We therefore studied the single-dose tolerability of KC2-SNALP in rats—a popular rodent model for assessing the toxicology of siRNA and nucleic acid-based therapeutics. As doses near the efficacious dose level were found to be very well tolerated (data not shown), single-dose escalation studies were conducted starting at doses ~50-fold higher (1 mg/kg) than the observed  $ED_{50}$  of the formulation. To understand formulation toxicity in the absence of any toxicity or pharmacologic effects resulting from target silencing, we conducted the experiments using a nontargeting control siRNA sequence directed against luciferase. KC2-SNALP containing luciferase siRNA was prepared in the exact same manner as that containing Factor VII siRNA, and the resultant size, lipid composition and entrapped siRNA/lipid ratio were similar. Clinical signs were observed daily and body weights, serum chemistry and hematology parameters were measured 72 h after dosing. KC2-SNALP was very well tolerated at the high dose levels examined (relative to the observed  $ED_{50}$  dose) with no dose-dependent, clinically significant changes in key serum chemistry or hematology parameters (**Table 2**).

Given the promising activity and safety profile observed in rodents, studies were initiated in nonhuman primates to investigate the translation of DLin-KC2-DMA activity in higher species. For these studies, we chose to target transthyretin (*TTR*), a hepatic gene of high therapeutic interest<sup>20</sup>. *TTR* is a serum protein synthesized primarily in the liver, and although amyloidogenic *TTR* mutations are rare, they are endemic to certain populations and can affect the peripheral nerves, leading to familial amyloidotic polyneuropathy, and the heart, leading to familial amyloid cardiomyopathy. Currently, the only disease-modifying therapy is liver transplantation. We treated cynomolgus monkeys with a single 15-min intravenous infusion of KC2-SNALP-formulated siTTR at siRNA doses of 0.03, 0.1, 0.3 and 1 mg/kg. Control animals received a single 15-min intravenous infusion of PBS or KC2-SNALP-formulated ApoB siRNA at a dose of 1 mg/kg. Tissues were harvested 48 h after administration and liver mRNA levels of *TTR* were determined. A clear dose response was obtained with an apparent  $ED_{50}$  of ~0.3 mg/kg (**Fig. 3b**). A toxicological analysis indicated that the treatment was well tolerated at the dose levels tested, with no treatment-related changes in animal appearance or behavior. No dose-dependent, clinically significant alterations in key clinical chemistry or hematological parameters were observed (**Supplementary Table 4**).

In summary, we applied a rational approach to the design of novel cationic lipids, which were screened for use in LNP-based siRNA delivery systems. Lipid structure was divided into three main functional elements: alkyl chain, linker and headgroup. With DLinDMA as a starting point, the effect of each of these elements was investigated in a systematic fashion, by holding the other two constant. First, the alkyl chains were established, then linker was varied and, finally, different headgroup structures were explored. Using this approach, important structure-activity considerations for ionizable cationic lipids were described and lipids with improved activity relative to the DLinDMA benchmark were identified. A SNALP formulation of the best-performing lipid (DLin-KC2-DMA) was well-tolerated in both rodent and nonhuman primates and exhibited *in vivo* activity at siRNA doses as low as 0.01 mg/kg in rodents, as well as silencing of a therapeutically significant gene (*TTR*) in nonhuman primates. Although the scope of the current work has been limited to hepatic delivery *in vivo*, the *TTR* silencing achieved in this work ( $ED_{50}$  ~ 0.3 mg/kg) represents a substantial improvement in activity relative to previous reports of LNP-siRNA mediated silencing in nonhuman primates.

## METHODS

Methods and any associated references are available in the online version of the paper at <http://www.nature.com/naturebiotechnology/>.

*Note: Supplementary information is available on the Nature Biotechnology website.*

## ACKNOWLEDGMENTS

The authors thank K. McClintock for assistance with animal studies. The authors also thank the Centre for Drug Research and Development at the University

of British Columbia for use of the NMR facilities and M. Heller for his expert assistance in setting up the  $^{31}\text{P}$ -NMR experiments.

#### AUTHOR CONTRIBUTIONS

J.C., M.A.C., P.R.C., T.D.M., M.J.H. and K.F.W. designed and advised on novel lipids. J.C., K.F.W. and M.S. synthesized novel lipids. M.J.H., T.D.M., J.C., K.F.W., M.M., K.G.R., M.A.M., M.T. and M.J. analyzed and interpreted lipid data. T.D.M., M.J.H. and M.A.T. co-directed novel lipid synthesis and screening program. S.C.S. designed and directed rodent *in vivo* studies. S.C.S., S.K.K., B.L.M., K.L., M.L.E., M.K., A.P.S., Y.K.T., S.A.B., W.L.C., M.J.W. and E.J.C. generated rodent *in vivo* data, including Factor VII and tolerability analyses. L.N., V.K., T.B., R.A., Q.C. and D.W.Y.S. developed novel siRNAs targeting *TTR*. R.A. and A.A. designed and directed NHP *in vivo* studies. S.C.S., S.K.K., A.A., B.L.M., I.M., A.P.S., Y.K.T., R.A., T.B., D.W.Y.S., S.A.B., J.Q., J.R.D. and A.d.F. analyzed and interpreted *in vivo* data. B.L.M., K.L., A.P.S., S.K.K., S.C.S. and E.J.C. generated and characterized preformed vesicle formulations with novel lipids. D.S. and C.K.C. developed methods and designed and conducted HPLC lipid analyses of preformed vesicle formulations. E.Y. and L.B.J. prepared SNALP formulations. P.R.C. directed biophysical studies and advised on methods. A.P.S., I.M.H., S.D. and K.W. performed biophysical characterization studies ( $pK_a$ , NMR, differential scanning calorimetric) of novel lipids and formulations. M.J.H., P.R.C., T.D.M., A.P.S., I.M.H. and K.F.W. analyzed biophysical data. S.C.S., M.J.H., A.A. and P.R.C. co-wrote the manuscript. T.D.M., M.M., M.A.M., M.A.T. and A.D.F. reviewed and edited the manuscript. S.C.S., M.J.H., A.A., P.R.C., I.M. and A.D.F. were responsible for approval of the final draft.

#### COMPETING INTERESTS STATEMENT

The authors declare competing financial interests: details accompany the full-text HTML version of the paper at <http://www.nature.com/naturebiotechnology/>.

Published online at <http://www.nature.com/naturebiotechnology/>.

Reprints and permissions information is available online at <http://npg.nature.com/reprintsandpermissions/>.

1. de Fougerolles, A.R. Delivery vehicles for small interfering RNA in vivo. *Hum. Gene Ther.* **19**, 125–132 (2008).
2. Whitehead, K.A., Langer, R. & Anderson, D.G. Knocking down barriers: advances in siRNA delivery. *Nat. Rev. Drug Discov.* **8**, 129–138 (2009).
3. Judge, A.D. *et al.* Confirming the RNAi-mediated mechanism of action of siRNA-based cancer therapeutics in mice. *J. Clin. Invest.* **119**, 661–673 (2009).

4. Judge, A.D. *et al.* Sequence-dependent stimulation of the mammalian innate immune response by synthetic siRNA. *Nat. Biotechnol.* **23**, 457–462 (2005).
5. Morrissey, D.V. *et al.* Potent and persistent *in vivo* anti-HBV activity of chemically modified siRNAs. *Nat. Biotechnol.* **23**, 1002–1007 (2005).
6. Zimmermann, T.S. *et al.* RNAi-mediated gene silencing in non-human primates. *Nature* **441**, 111–114 (2006).
7. Akinc, A. *et al.* A combinatorial library of lipid-like materials for delivery of RNAi therapeutics. *Nat. Biotechnol.* **26**, 561–569 (2008).
8. Frank-Kamenetsky, M. *et al.* Therapeutic RNAi targeting PCSK9 acutely lowers plasma cholesterol in rodents and LDL cholesterol in nonhuman primates. *Proc. Natl. Acad. Sci. USA* **105**, 11915–11920 (2008).
9. Hafez, I.M., Maurer, N. & Cullis, P.R. On the mechanism whereby cationic lipids promote intracellular delivery of polynucleic acids. *Gene Ther.* **8**, 1188–1196 (2001).
10. Xu, Y. & Szoka, F.C. Jr. Mechanism of DNA release from cationic liposome/DNA complexes used in cell transfection. *Biochemistry* **35**, 5616–5623 (1996).
11. Zelphati, O. & Szoka, F.C. Jr. Mechanism of oligonucleotide release from cationic liposomes. *Proc. Natl. Acad. Sci. USA* **93**, 11493–11498 (1996).
12. Torchilin, V.P. Recent approaches to intracellular delivery of drugs and DNA and organelle targeting. *Annu. Rev. Biomed. Eng.* **8**, 343–375 (2006).
13. Semple, S.C. *et al.* Efficient encapsulation of antisense oligonucleotides in lipid vesicles using ionizable aminolipids: formation of novel small multilamellar vesicle structures. *Biochim. Biophys. Acta* **1510**, 152–166 (2001).
14. Maurer, N. *et al.* Spontaneous entrapment of polynucleotides upon electrostatic interaction with ethanol-destabilized cationic liposomes. *Biophys. J.* **80**, 2310–2326 (2001).
15. Heyes, J., Palmer, L., Bremner, K. & MacLachlan, I. Cationic lipid saturation influences intracellular delivery of encapsulated nucleic acids. *J. Control. Release* **107**, 276–287 (2005).
16. Semple, S.C., Chonn, A. & Cullis, P.R. Interactions of liposomes and lipid-based carrier systems with blood proteins: Relation to clearance behaviour in vivo. *Adv. Drug Deliv. Rev.* **32**, 3–17 (1998).
17. Bailey, A.L. & Cullis, P.R. Modulation of membrane fusion by asymmetric transbilayer distributions of amino lipids. *Biochemistry* **33**, 12573–12580 (1994).
18. Cullis, P.R. & de Kruijff, B. The polymorphic phase behaviour of phosphatidyl-ethanolamines of natural and synthetic origin. A  $^{31}\text{P}$  NMR study. *Biochim. Biophys. Acta* **513**, 31–42 (1978).
19. Epand, R.F., Robinson, K.S., Andrews, M.E. & Epand, R.F. Dependence of the bilayer to hexagonal phase transition on amphiphile chain length. *Biochemistry* **28**, 9398–9402 (1989).
20. Sekijima, Y., Kelly, J.W. & Ikeda, S. Pathogenesis of and therapeutic strategies to ameliorate the transthyretin amyloidoses. *Curr. Pharm. Des.* **14**, 3219–3230 (2008).
21. Cullis, P.R., Hope, M.J. & Tilcock, C.P. Lipid polymorphism and the roles of lipids in membranes. *Chem. Phys. Lipids* **40**, 127–144 (1986).



## ONLINE METHODS

**Synthesis of cationic and PEG-lipids.** A detailed description of the cationic lipid syntheses is available in the **Supplementary Syntheses 1 and 2**. The synthesis of N-[(methoxy poly(ethylene glycol)<sub>2000</sub>carbamoyl]-1,2-dimyrityloxypropyl-3-amine (PEG-C-DMA) was as described<sup>22</sup>. The synthesis of R-3-[( $\omega$ -methoxy poly(ethylene glycol)<sub>2000</sub>carbamoyl)]-1,2-dimyrityloxypropyl-3-amine (PEG-C-DOMG) was as described<sup>7</sup>. These lipids were interchangeable in the formulation without substantially affecting activity (data not shown), and are collectively referred to as PEG-lipid.

**siRNA synthesis.** All siRNAs were synthesized by Alnylam and were characterized by electrospray mass spectrometry and anion exchange high-performance liquid chromatography (HPLC). The sequences for the sense and antisense strands of Factor VII, ApoB and control siRNAs have been reported<sup>7</sup>. The sequences for the sense and antisense strands of the TTR siRNA is as follows:

siTTR sense: 5'-GuAAccAAGAGuAuuccAudTdT-3'; antisense: 5'-AUGGAAuACUCUUGGUuACdTdT-3'.

2'-O-Me-modified nucleotides are in lowercase. siRNAs were generated by annealing equimolar amounts of complementary sense and antisense strands.

**Preformed vesicle method to formulate LNP-siRNA systems.** LNP-siRNA systems were made using the preformed vesicle method<sup>14</sup>. Cationic lipid, DSPC, cholesterol and PEG-lipid were solubilized in ethanol at a molar ratio of 40:10:40:10, respectively. The lipid mixture was added to an aqueous buffer (50 mM citrate, pH 4) with mixing to a final ethanol and lipid concentration of 30% (vol/vol) and 6.1 mg/ml, respectively, and allowed to equilibrate at 22 °C for 2 min before extrusion. The hydrated lipids were extruded through two stacked 80 nm pore-sized filters (Nuclepore) at 22 °C using a Lipex Extruder (Northern Lipids) until a vesicle diameter of 70–90 nm, as determined by dynamic light scattering analysis, was obtained. This generally required 1–3 passes. The siRNA (solubilized in a 50 mM citrate, pH 4 aqueous solution containing 30% ethanol) was added to the pre-equilibrated (35 °C) vesicles at a rate of ~5 ml/min with mixing. After a final target siRNA/lipid ratio of 0.06 (wt/wt) was reached, the mixture was incubated for a further 30 min at 35 °C to allow vesicle reorganization and encapsulation of the siRNA. The ethanol was then removed and the external buffer replaced with PBS (155 mM NaCl, 3 mM Na<sub>2</sub>HPO<sub>4</sub>, 1 mM KH<sub>2</sub>PO<sub>4</sub>, pH 7.5) by either dialysis or tangential flow diafiltration.

**Preparation of KC2-SNALP.** siRNA were encapsulated in SNALP using a controlled step-wise dilution method process as described<sup>23</sup>. The lipid constituents of KC2-SNALP were DLin-KC2-DMA (cationic lipid), dipalmitoylphosphatidylcholine (DPPC; Avanti Polar Lipids), synthetic cholesterol (Sigma) and PEG-C-DMA used at a molar ratio of 57.1:7.1:34.3:1.4. Upon formation of the loaded particles, SNALP were dialyzed against PBS and filter sterilized through a 0.2  $\mu$ m filter before use. Mean particle sizes were 75–85 nm and 90–95% of the siRNA was encapsulated within the lipid particles. The final siRNA/lipid ratio in formulations used for *in vivo* testing was ~0.15 (wt/wt).

***In vivo* screening of cationic lipids for Factor VII activity.** Eight- to 10-week-old, female C57BL/6 mice were obtained from Harlan. Mice were held in a pathogen-free environment and all procedures involving animals were performed in accordance with local, state and federal regulations, as applicable, and approved by the Institutional Animal Care and Use Committee (IACUC). LNP-siRNA systems containing Factor VII siRNA were diluted to the appropriate concentrations in sterile PBS immediately before use and the formulations were administered intravenously through the lateral tail vein in a total volume of 10 ml/kg. After 24 h, animals were anesthetized with ketamine/xylazine and blood was collected by cardiac puncture and processed to serum (microtainer serum separator tubes; Becton Dickinson). Serum was tested immediately or stored at -70 °C for later analysis for Factor VII levels.

**Measurement of Factor VII protein in serum.** Serum Factor VII levels were determined using the colorimetric Biophen VII assay kit (Aniara)<sup>7</sup>. Briefly, serially diluted pooled control serum (200–3.125%) and appropriately

diluted serum samples from treated animals ( $n = 4$ –5 animals per dose level) were analyzed in 96-well, flat bottom, nonbinding polystyrene assay plates (Corning) using the Biophen VII kit according to manufacturer's instructions. Absorbance was measured at 405 nm and a calibration curve was generated using the serially diluted control serum to determine levels of Factor VII in serum from treated animals, relative to the saline-treated control animals. ED<sub>50</sub> values for each formulation were derived from linear interpolation of the Factor VII activity profile, and included data points within 10–90% residual Factor VII activity (typically three to six points). Formulations containing novel lipids were always screened with one or more benchmark formulations to control and assess assay variability over time, and formulations with promising activity were repeated, with an expanded number of dose levels.

***In situ* determination of pK<sub>a</sub> using TNS.** The pK<sub>a</sub> of each cationic lipid was determined in LNPs using TNS<sup>17</sup> and preformed vesicles composed of cationic lipid/DSPC/cholesterol/PEG-lipid (40:10:40:10 mol%) in PBS at a concentration of ~6 mM total lipid. TNS was prepared as a 100  $\mu$ M stock solution in distilled water. Vesicles were diluted to 100  $\mu$ M lipid in 2 ml of buffered solutions containing 1  $\mu$ M TNS, 10 mM HEPES, 10 mM 4-morpholineethanesulfonic acid, 10 mM ammonium acetate, 130 mM NaCl, where the pH ranged from 2.5 to 11. Fluorescence intensity was monitored in a stirred, thermostated cuvette (25 °C) in a PerkinElmer LS-50 Spectrophotometer using excitation and emission wavelengths of 321 nm and 445 nm. Fluorescence measurements were made 30 s after the addition of the lipid to the cuvette. A sigmoidal best fit analysis was applied to the fluorescence data and the pK<sub>a</sub> was measured as the pH giving rise to half-maximal fluorescence intensity.

**Differential scanning calorimetry.** Analyses were performed using the same samples used for <sup>31</sup>P NMR, on a TA Instruments Q2000 calorimeter using a heat/cool/heat cycle and a scan rate of 1 °C/minute between 10 °C and 70 °C. Repeat scans were reproducible to within 0.1 °C. The temperature at the peak amplitude of the endo- and exotherms was measured for both the heating and cooling scans, and the T<sub>BH</sub> values observed correlated closely with the phase transition temperatures measured using <sup>31</sup>P NMR.

**Determination of siRNA plasma levels.** Plasma levels of fluorescently labeled Cy3 siRNA were evaluated at 0.5 and 3 h after intravenous injection of selected LNP (preformed vesicle) formulations, administered at an siRNA dose of 5 mg/kg, in C57BL/6 mice. Blood was collected in EDTA-containing Vacutainer tubes, processed to plasma at 2–8 °C, and either assayed immediately or stored at -30 °C. An aliquot of the plasma (100  $\mu$ l maximum) was diluted to 500  $\mu$ l with PBS (145 mM NaCl, 10 mM phosphate, pH 7.5); methanol (1.05 ml) and chloroform (0.5 ml) were added; and the sample was vortexed to obtain a clear, single-phase solution. Additional water (0.5 ml) and chloroform (0.5 ml) was added and the resulting emulsion was sustained by periodic mixing. The mixture was centrifuged at 500g for 20 min and the aqueous phase containing the Cy3-labeled siRNA was collected and the fluorescence measured using an SLM Fluorimeter at an excitation wavelength of 550 nm (2 nm bandwidth) and emission wavelength of 600 nm (16 nm bandwidth). A standard curve was generated by spiking aliquots of plasma from untreated animals with the formulation containing Cy-3-siRNA (0 to 15  $\mu$ g/ml), and the resulting standards were processed as indicated above.

**Determination of siRNA biodistribution.** Tissue (liver and spleen) levels of siRNA were evaluated at 0.5 and 3 h after intravenous injection in C57BL/6 mice after administration of LNP (preformed vesicle) formulations containing selected novel lipids. After blood collection, animals were perfused with saline to remove residual blood from the tissues; liver and spleen were then collected, weighed and divided into two pieces. Portions (400–500 mg) of liver or whole spleens were weighed into Fastprep tubes and homogenized in 1 ml of Trizol using a Fastprep FP120 instrument. An aliquot of the homogenate (typically equivalent to 50 mg of tissue) was transferred to an Eppendorf tube and additional Trizol was added to achieve a final volume of 1 ml. Chloroform (0.2 ml) was added and the solution was mixed and incubated for 2–3 min, before being centrifuged for 15 min at 12,000g. An aliquot (0.5 ml) of the aqueous phase was diluted with 0.5 ml of PBS and the

sample fluorescence was measured as described above. The data were expressed as the percent of the injected dose (in each tissue).

***In vivo nonhuman primate experiments.*** All procedures using cynomolgus monkeys were conducted by a certified contract research organization using protocols consistent with local, state and federal regulations, as applicable, and approved by the IACUC. Cynomolgus monkeys ( $n = 3$  per group) received either 0.03, 0.1, 0.3 or 1 mg/kg siTTR, or 1 mg/kg siApoB (used as control) formulated in KC2-SNALP as 15-min intravenous infusions (5 ml/kg) through the cephalic vein. Animals were euthanized 48 h after administration, and a 0.15–0.20 g sample of the left lateral lobe of the liver was collected and snap-frozen in liquid nitrogen. Prior studies have established uniformity of silencing activity throughout the liver<sup>6</sup>. *TTR* mRNA levels, relative to *GAPDH*

mRNA levels, were determined in liver samples using a branched DNA assay (QuantiGene Assay)<sup>6</sup>. Clinical chemistry and hematology parameters were analyzed before and 48 h after administration.

**Statistical analysis.** *P*-values were calculated for comparison of K2C-SNALP-treated animals with PBS-treated animals using analysis of variance (ANOVA, single-factor) with an alpha value of 0.05.  $P < 0.05$  was considered significant.

22. Heyes, J., Hall, K., Taylor, V., Lenz, R. & MacLachlan, I. Synthesis and characterization of novel poly(ethylene glycol)-lipid conjugates suitable for use in drug delivery. *J. Control. Release* **112**, 280–290 (2006).
23. Jeffs, L.B. *et al.* A scalable, extrusion-free method for efficient liposomal encapsulation of plasmid DNA. *Pharm. Res.* **22**, 362–372 (2005).